

## Electrically driven spin polarization in $\text{Pr}_{0.7}\text{Ca}_{0.3}\text{MnO}_3/\text{YBa}_2\text{Cu}_3\text{O}_7$ heterostructures

J. G. Lin, Daniel Hsu, C. H. Chiang, and W. C. Chan

Citation: *Journal of Applied Physics* **105**, 07E301 (2009); doi: 10.1063/1.3055269

View online: <http://dx.doi.org/10.1063/1.3055269>

View Table of Contents: <http://scitation.aip.org/content/aip/journal/jap/105/7?ver=pdfcov>

Published by the [AIP Publishing](#)

---

### Articles you may be interested in

Effect of current induced charge-order melting of  $\text{Pr}_{0.5}\text{Ca}_{0.5}\text{MnO}_3$  in partially masked superconducting  $\text{Pr}_{0.5}\text{Ca}_{0.5}\text{MnO}_3/\text{YBa}_2\text{Cu}_3\text{O}_7$  bilayer

*J. Appl. Phys.* **114**, 233901 (2013); 10.1063/1.4848103

The effects of strain, current, and magnetic field on superconductivity in  $\text{Pr}_{0.5}\text{Ca}_{0.5}\text{MnO}_3/\text{YBa}_2\text{Cu}_3\text{O}_7/\text{Pr}_{0.5}\text{Ca}_{0.5}\text{MnO}_3$  trilayer

*J. Appl. Phys.* **113**, 113902 (2013); 10.1063/1.4795349

Effect of current induced charge order melting of  $\text{Pr}_{0.5}\text{Ca}_{0.5}\text{MnO}_3$  on  $\text{YBa}_2\text{Cu}_3\text{O}_7$  thin film

*AIP Conf. Proc.* **1447**, 675 (2012); 10.1063/1.4710183

Evolution of ferromagnetic clustering in  $\text{Pr}_{0.5}\text{Ca}_{0.5}\text{MnO}_3$  and its effect on the critical temperature of  $\text{YBa}_2\text{Cu}_3\text{O}_7$  thin film

*J. Appl. Phys.* **111**, 113910 (2012); 10.1063/1.4725422

Current enhanced magnetic proximity in  $\text{Nd}_{0.7}\text{Ca}_{0.3}\text{MnO}_3/\text{YBa}_2\text{Cu}_3\text{O}_7$  bilayer

*Appl. Phys. Lett.* **90**, 162504 (2007); 10.1063/1.2722673

---

A promotional banner for the 2014 Special Topics in AIP Materials. The banner has an orange background with a white border. At the top, the text '2014 Special Topics' is written in a large, white, sans-serif font. Below this, there are five circular icons, each containing a different material structure and a label: 'PEROVSKITES' (red and black geometric shapes), '2D MATERIALS' (blue and red hexagonal lattice), 'MESOPOROUS MATERIALS' (green and blue porous structure), 'BIOMATERIALS/ BIOELECTRONICS' (yellow and black structure), and 'METAL-ORGANIC FRAMEWORK MATERIALS' (brown and black structure). At the bottom left, the 'AIP | APL Materials' logo is displayed. At the bottom right, a red banner with white text says 'Submit Today!'.

# Electrically driven spin polarization in $\text{Pr}_{0.7}\text{Ca}_{0.3}\text{MnO}_3/\text{YBa}_2\text{Cu}_3\text{O}_7$ heterostructures

J. G. Lin,<sup>1,a)</sup> Daniel Hsu,<sup>1</sup> C. H. Chiang,<sup>2</sup> and W. C. Chan<sup>2</sup>

<sup>1</sup>*Center for Condensed Matter Sciences, National Taiwan University, Taipei, 106 Taiwan, Republic of China*

<sup>2</sup>*Department of Physics, Tamkang University, Tamsui, Taipei, 251 Taiwan, Republic of China*

(Presented 13 November 2008; received 4 September 2008; accepted 2 October 2008; published online 29 January 2009)

The current and temperature dependent electrical transport is investigated in  $\text{Pr}_{0.7}\text{Ca}_{0.3}\text{MnO}_3/\text{YBa}_2\text{Cu}_3\text{O}_7$  (PCMO/YBCO) heterostructures which are fabricated by pulsed laser deposition. Two PCMO/YBCO heterostructures are made with the thicknesses of PCMO varied. It is shown that the superconducting transition temperature significantly decreases with increasing thickness of PCMO and with increasing applied current, which are related to the pair breaking via the polarized electrons. However, the current-dependent normal-state resistivity shows two crossing points, indicating the competition of various phases. According to our analysis, the melting of charge ordering state by the electrical current may be the major cause for the electrically driven enhancement of spin polarization in PCMO/YBCO. © 2009 American Institute of Physics. [DOI: 10.1063/1.3055269]

## I. INTRODUCTION

Materials with possible applications of spin-injection devices in the field of “spintronics” have received a lot of attention in the recent years.<sup>1–3</sup> Such devices can be realized in various heterostructures consisted of superconductor and ferromagnet. For example, the spin valve system consisted of a superconducting (SC) layer sandwiched between two ferromagnetic (FM) layers requires an antiferromagnetic (AFM) interlayer to pin the spins of one of the FM layers. Therefore, the understanding of proximity effect in AFM/SC as well as FM/SC system is important toward the realization of such devices. Among them, the hybrid transition-metal oxides such as high temperature superconductor (HTSC) (Ref. 4) and colossal-magnetoresistance manganites (CMRMs) generate a great deal of attraction.<sup>5</sup> The studies on the CMRM/HTSC heterostructures are motivated not only because of their potential for the new devices but also the interesting physics behind.<sup>6–13</sup> In the half-metallic ferromagnets of nearly 100% spin polarization at the Fermi level, such as  $\text{La}_{0.7}\text{Ca}_{0.3}\text{MnO}_3$ , the diffusion length (DL) of the superconducting pairs of  $\text{YBa}_2\text{Cu}_3\text{O}_7$  (YBCO) is relatively short ( $\sim 30$  nm). However, when YBCO hybridizes with an insulating AFM manganite such as  $\text{Nd}_{0.7}\text{Ca}_{0.3}\text{MnO}_3$  (NCMO), DL is relatively long ( $> 200$  nm). In this work, the polarization-related transport properties of  $\text{Pr}_{0.7}\text{Ca}_{0.3}\text{MnO}_3$  (PCMO)/YBCO heterostructure are studied and the results are compared with that of NCMO/YBCO. By comparing these two analogous systems, the mechanism of electrically driven spin injection in CMRM/HTSC hybrid oxides can be further understood.<sup>14</sup>

## II. EXPERIMENT

The PCMO, YBCO, and PCMO/YBCO films were deposited on  $\text{LaAlO}_3$  single crystal substrate by pulsed laser deposition system with a KrF (248 nm) laser. All the PCMO, YBCO, and PCMO/YBCO bilayers were epitaxially grown in the flowing  $\text{O}_2$  of 50 mTorr at the temperatures of 800 and 850 °C for PCMO and YBCO, respectively. In addition, the YBCO and PCMO samples were postannealed at 400 °C for 60 min under an oxygen pressure of 300 Torr. The thicknesses of two PCMO/YBCO samples, determined from the deposition time, were 80/160 nm and 160/160 nm with respect to the samples P/Y(1) and P/Y(2). The phase purity of all the films was analyzed by x-ray diffraction (XRD) using Bruker D8 machine. dc magnetization and magnetic hysteresis loops were measured with the applied field parallel to the film surface using a SQUID magnetometer (Quantum Design). Temperature dependent resistivity measurements with different applying currents were carried out with a standard four-probe configuration in a closed-cycle refrigerator system. Keithley 220 and 182 were used as the current source and the voltage meter, respectively.

## III. RESULTS AND DISCUSSION

The XRD patterns exhibit only the corresponding (00 $l$ ) peaks for YBCO, PCMO, and the  $\text{LaAlO}_3$  substrate as shown in Fig. 1, indicating good crystalline structures with a preferential growth along the  $c$ -axis. In particular, PCMO/YBCO heterostructures contain all the indexed XRD lines corresponding to the single layers, confirming the phase purity and the formation of epitaxial structure.

Figure 2(a) presents the magnetization ( $M$ ) vs temperature ( $T$ ) for PCMO film under zero-field-cooled (ZFC) and field-cooled (FC) modes with an applied field of 100 Oe. The  $M$ - $T$  curves shows the canted AFM phase at  $T \sim 110$  K which is comparable to the value of single crystal.<sup>15</sup> How-

<sup>a)</sup>Author to whom correspondence should be addressed. Electronic mail: jglin@ntu.edu.tw.

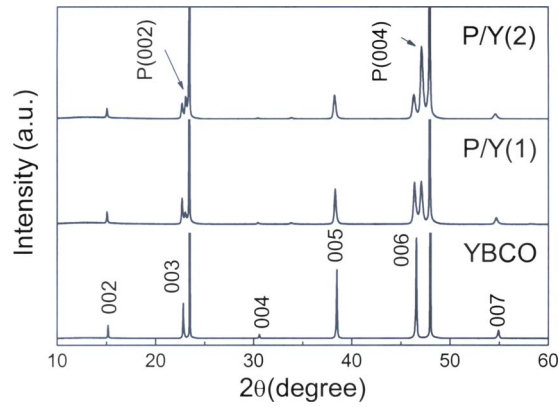


FIG. 1. (Color online) The XRD patterns of YBCO single layer and PCMO/YBCO heterostructures. All the peaks are identified as (00l).

ever, the charge ordering transition temperature  $T_{co}$  cannot be clearly observed from the  $M(T)$  curves. The inset of Fig. 2(a) is the  $\rho$ - $T$  curve of PCMO film, showing that an insulating-like behavior is observed. The magnitude of  $\rho(T)$  decreases with the applied current  $> 1$  mA, which is likely to the melting of charge ordering (CO). Figure 2(b) is the plot of  $M$ - $T$  for YBCO film, the diamagnetic behavior can be observed and the superconducting transition temperature  $T_{sc}$  is defined as 88 K which is close to the value measured from the  $\rho$ - $T$  curve in the inset of Fig. 2(b).

Figure 3 shows the  $M$ - $T$  curves of P/Y(1) under ZFC and FC modes. Based on the  $M$ - $T$  curves,  $T_{sc}$  is determined as 70 K which is 18 K lower than that of YBCO film. The  $M$ - $H$  hysteresis loop at  $T=50$  K for P/Y(1) is shown in the inset of Fig. 3. This plot clearly demonstrates a superconducting state with a finite pinning force.

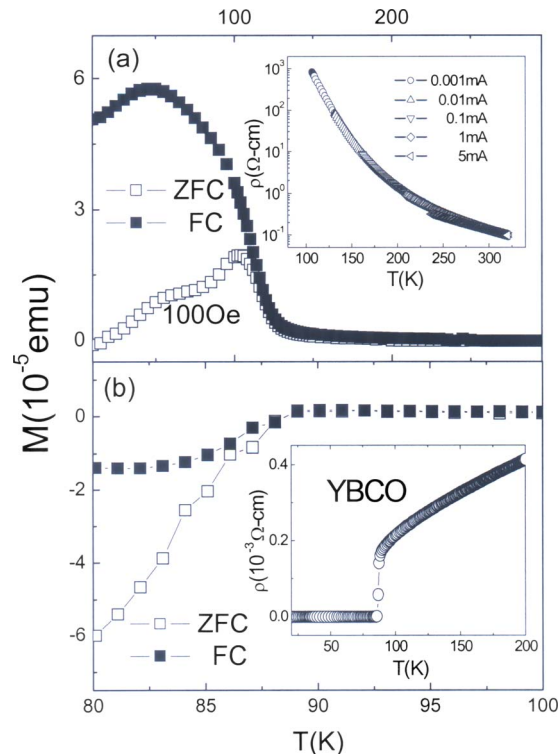


FIG. 2. (Color online)  $M(T)$  for (a) PCMO and (b) YBCO film under the ZFC and FC modes. The insets are the  $\rho(T)$  curves for PCMO and YBCO, respectively.

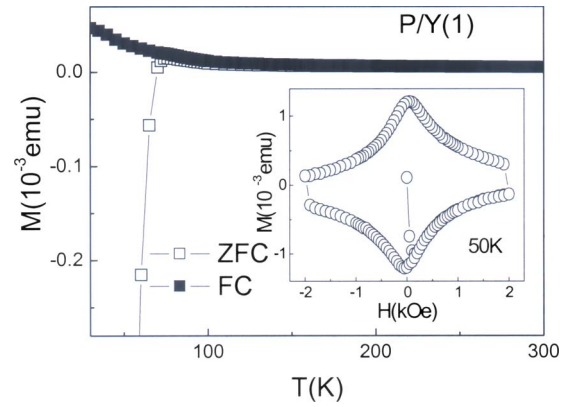


FIG. 3. (Color online)  $M(T)$  for P/Y(1) under ZFC and FC modes. The inset is the  $M$ - $H$  curves for P/Y(1) measured at 50 K.

The  $\rho(T)$  for P/Y(1) and P/Y(2) are plotted in Fig. 4 with various current  $I$  from 0.1 to 50 mA. The behavior of  $\rho(T)$  in P/Y(1) and P/Y(2) is different from those of pure YBCO and PCMO, implying that the bilayer sample has its unique electronic structure.  $T_{sc}$  decreases to about 64 and 47 K for P/Y(1) and P/Y(2), respectively. Moreover, with increasing  $I$ ,  $T_{sc}$  decreases monotonically but not linearly, as seen from the inset of Figs. 4(a) and 4(b). Interestingly, in the normal state there are two crossing points in these curves, which behavior is different from the observed single crossing point in the  $\rho(T)$  curves of NCMO/YBCO bilayers.<sup>16,17</sup> For P/Y(1), the

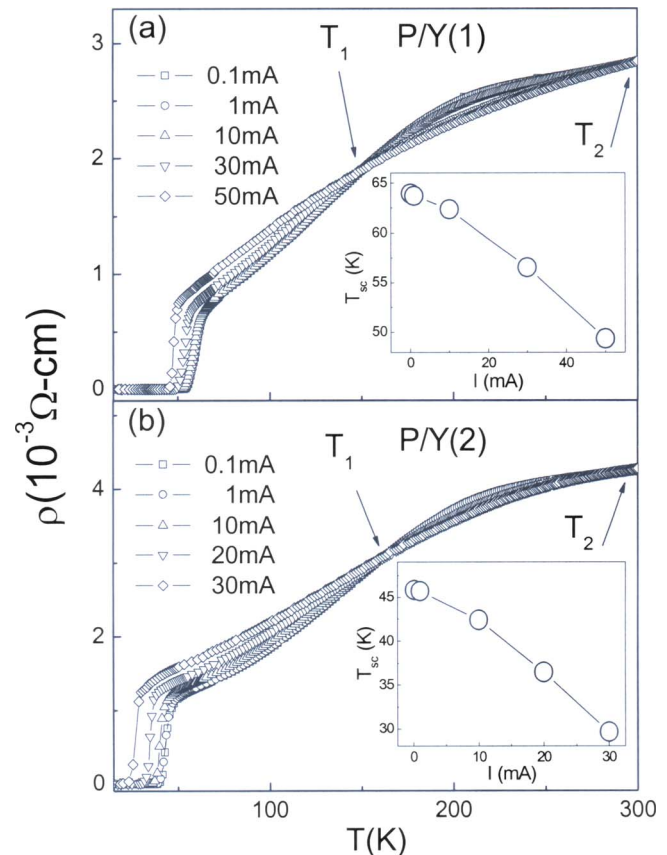


FIG. 4. (Color online)  $\rho(T)$  curves for (a) P/Y(1) and (b) P/Y(2) with different applied current from 0.1 to 50 mA. The arrows note the crossing points of curves. The insets show the  $T_{sc}$  as functions of applying current.

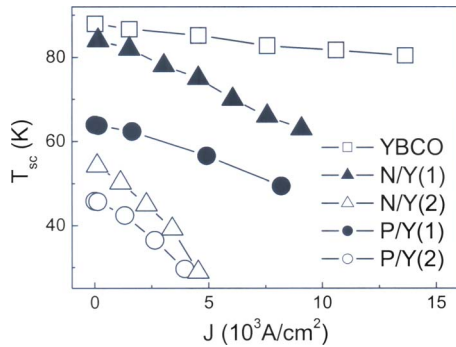


FIG. 5. (Color online)  $T_{sc}$  vs current density for YBCO, N/Y(1), N/Y(2), P/Y(1), and P/Y(2), where N/Y(1) and N/Y(2) represent samples of NCMO(100 nm)/YBCO(200 nm) and NCMO(200 nm)/YBCO(200 nm) respectively, as referred in Ref. 14.

crossing points occur at around 152 and 300 K, which are marked as  $T_1$  and  $T_2$ . While for P/Y(2), the values of  $T_1$  and  $T_2$  are 162 and 300 K, respectively. The crossing behavior can be viewed as the competition between different phases. First crossing point is that between insulating and metallic phases, and the second one is that between superconducting and metallic phases.

Figure 5 is a plot of  $T_{sc}$  versus applied current density ( $J$ ) for YBCO single layer and PCMO/YBCO bilayers, together with our previous results of NCMO/YBCO bilayers. The denotations of N/Y(1) and N/Y(2) in Fig. 5 represent samples of NCMO(100 nm)/YBCO(200 nm) and NCMO(200 nm)/YBCO(200 nm), respectively, as referred in Ref. 14. It indicates that the rate of current-induced  $T_{sc}$  suppression ( $dT_{sc}/dJ$ ) is roughly around  $4.55 \times 10^{-4}$  K/A cm<sup>-2</sup> for YBCO,  $1.80 \times 10^{-3}$  K/A cm<sup>-2</sup> for P/Y(1), and  $4.45 \times 10^{-3}$  K/A cm<sup>-2</sup> for P/Y(2) which is one order larger than that in YBCO but slightly lower than those of NCMO/YBCO bilayers. In principle, the mechanism of current-induced  $T_{sc}$  suppression by ordinary quasiparticles is a pair-breaking effect due to the perturbation of superconducting order parameter. However, when the electrons flows through PCMO and are polarized, they introduce an extra spin-flip effect, results in an enhancement of pair breaking. Therefore, the current-dependent  $T_{sc}$  suppression rate should be proportional to the degree of spin polarization. Since the CO dominates the insulating AFM phase at low temperature, it is very likely that current melts the CO state and enhances the spin polarization. This physical picture is consistent with the fact that the CO state exist in both NCMO and PCMO and their behaviors of current-dependent  $T_{sc}$  suppression are rather similar.

#### IV. CONCLUSION

In conclusion, the current and temperature dependences of resistivity for PCMO/YBCO bilayers are investigated. Our results demonstrate that the current-induced suppression rates of the superconducting transition temperature are one order larger in PCMO/YBCO than that in pure YBCO film, suggesting a significant effect of pair breaking by the polarized quasiparticles. Furthermore, two crossing points in the current-dependent resistivity curves are observed, suggesting a competition between various phases. Based on our analysis, the melting of charge ordering state should be the major mechanism for the enhancement of electrically driven spin polarization.

#### ACKNOWLEDGMENT

This work is supported by the National Science Council of ROC (NSC-96-2112-M-002-027-MY3).

- <sup>1</sup>S. A. Wolf, D. D. Awschalom, R. A. Buhrman, J. M. Daughton, S. von Molnár, M. L. Roukes, A. Y. Chtchelkanova, and D. M. Treger, *Science* **294**, 1488 (2001).
- <sup>2</sup>G. Sun, D. Y. Xing, and J. Dong, *Phys. Rev. B* **65**, 174508 (2002).
- <sup>3</sup>T. Kontos, M. Aprili, J. Lesueur, and X. Grisson, *Phys. Rev. Lett.* **86**, 304 (2001).
- <sup>4</sup>M. K. Wu, J. R. Ashburn, C. J. Torng, P. H. Hor, R. L. Meng, L. Gao, Z. J. Huang, Y. Q. Wang, and C. W. Chu, *Phys. Rev. Lett.* **58**, 908 (1987).
- <sup>5</sup>R. Von Helmolt, J. Wecker, B. Hozzapfel, L. Schultz, and K. Samwer, *Phys. Rev. Lett.* **71**, 2331 (1993).
- <sup>6</sup>J. Y. T. Wei, N.-C. Yeh, and R. P. Vasquez, *Phys. Rev. Lett.* **79**, 5150 (1997).
- <sup>7</sup>V. A. Vas'ko, V. A. Larkin, P. A. Kraus, K. R. Nikolaev, D. E. Grupp, C. A. Nordman, and A. M. Goldman, *Phys. Rev. Lett.* **78**, 1134 (1997).
- <sup>8</sup>P. Mikheenko, M. S. Colclough, C. Severac, R. Chakalov, F. Welhoffer, and C. M. Muirhead, *Appl. Phys. Lett.* **78**, 356 (2001).
- <sup>9</sup>Z. Sefrioui, M. Varela, V. Pena, D. Arias, C. Leon, J. Santamaria, J. E. Villegas, J. L. Martinez, W. Saldarriaga, and P. Prieto, *Appl. Phys. Lett.* **81**, 4568 (2002).
- <sup>10</sup>S. Soltan, J. Albrecht, and H.-U. Haberman, *Phys. Rev. B* **70**, 144517 (2004).
- <sup>11</sup>Z. Chen, A. Biswas, I. Zutic, T. Wu, S. B. Ogale, R. L. Greene, and T. Venkatesan, *Phys. Rev. B* **63**, 212508 (2001).
- <sup>12</sup>J. Stahn, J. Chakhalian, Ch. Niedermayer, J. Hoppler, T. Gutberlet, J. Voigt, F. Treubel, H.-U. Haberman, G. Cristiani, B. Keimer, and C. Bernhard, *Phys. Rev. B* **71**, 140509(R) (2005).
- <sup>13</sup>J. G. Lin, S. L. Cheng, C. R. Chang, and D. Y. Xing, *J. Appl. Phys.* **97**, 113528 (2005).
- <sup>14</sup>Daniel Hsu, J. G. Lin, C. P. Chang, C. H. Chen, W. F. Wu, C. H. Chiang, and W. C. Chan, *J. Appl. Phys.* **103**, 07C710 (2008).
- <sup>15</sup>Y. Tomioka, A. Asamitsu, H. Kuwahara, Y. Moritomo, and Y. Tokura, *Phys. Rev. B* **53**, R1689 (1996).
- <sup>16</sup>Daniel Hsu, J. G. Lin, C. P. Chang, C. H. Chen, W. F. Wu, C. H. Chiang, and W. C. Chan, *Appl. Phys. Lett.* **90**, 162504 (2007).
- <sup>17</sup>J. G. Lin, Daniel Hsu, W. F. Wu, C. H. Chiang, and W. C. Chan, *J. Appl. Phys.* **101**, 09G106 (2007).